Published in final edited form as:

J Mol Cell Cardiol. 2018 January ; 114: 354–363. doi:10.1016/j.yjmcc.2017.12.005.

Absence of synemin in mice causes structural and functional abnormalities in heart

Karla P. García-Pelagio[a,b], **Ling Chen**[a,c], **Humberto C. Joca**[d,e], **Christopher Ward**[f], **W. Jonathan Lederer**[a,d], **Robert J. Bloch**[a,*]

[a]Department of Physiology, School of Medicine, University of Maryland, 655 W. Baltimore St., Baltimore, MD 21201, USA

[b]Department of Physics, School of Science, Universidad Nacional Autónoma de México, Av. Universidad 3000, Mexico City 04320, Mexico

[c]Department of Medicine, School of Medicine, University of Maryland, 655 W. Baltimore St., Baltimore, MD 21201, USA

[d]BioMET, University of Maryland, 111 S Penn St, Baltimore, MD 21201, USA

[e]Department of Biochemistry and Immunology, Institute of Biological Sciences, Universidade Federal de Minas Gerais, Av Prof. Alfredo Balena, 190, Belo Horizonte, MG 30130, Brazil

[f]School of Nursing and Department of Orthopedics, School of Medicine, University of Maryland,100 Penn St, Baltimore, MD 21201, USA

Abstract

Cardiomyopathies have been linked to changes in structural proteins, including intermediate filament (IF) proteins located in the cytoskeleton. IFs associate with the contractile machinery and costameres of striated muscle and with intercalated disks in the heart. Synemin is a large IF protein that mediates the association of desmin with Z-disks and stabilizes intercalated disks. It also acts as an A-kinase anchoring protein (AKAP). In murine skeletal muscle, the absence of synemin causes a mild myopathy. Here, we report that the genetic silencing of synemin in mice (synm −/−) causes left ventricular systolic dysfunction at 3 months and 12–16 months of age, and left ventricular hypertrophy and dilatation at 12–16 months of age. Isolated cardiomyocytes showed alterations in calcium handling that indicate defects intrinsic to the heart. Although contractile and costameric proteins remained unchanged in the old synm −/− hearts, we identified alterations in several signaling proteins (PKA-RII, ERK and p70S6K) critical to cardiomyocyte function. Our data suggest that synemin plays an important regulatory role in the heart and that the consequences of its absence are profound.

*Corresponding author. rbloch@som.umaryland.edu (R.J. Bloch).

Supplementary data to this article can be found online at https://doi.org/10.1016/j.yjmcc.2017.12.005.

Disclosures

None.

Keywords

Costameres; Intermediate filament; AKAPs; Hypertrophic and dilated cardiomyopathy; Muscular dystrophy

1. Introduction

Heart diseases are the leading cause of death globally, affecting 1 in every 3 deaths [1,2]. Cardiomyopathy (CM) represents a collection of diverse abnormal conditions of the heart muscle having as a common denominator the reduced ability of the heart to pump blood. Dilated and hypertrophic myopathies are the most common forms of CM.

Dilated cardiomyopathy (DCM) is characterized by enlargement of the ventricles, thinning of the ventricular wall, non-specific histological features, increased diastolic and systolic volumes and a low ejection fraction [3,4]. Fifteen genes related to DCM are associate with defects in sarcomeric, sarcolemmal and cytoskeletal proteins, such as dystrophin, desmin, titin and myosin [4,5].

Hypertrophic cardiomyopathy (HCM) is characterized by heart remodeling, increased heart mass and abnormal diastolic function that result in heart failure and premature death [3,6]. Genes related to HCM typically encode contractile proteins which play important roles in force generation [7–9].

All 3 major elements of the cytoskeleton – intermediate filaments (IFs), microfilaments, and microtubules — play important roles in striated muscle, with the IFs being the most resistant to strain and thus most likely to play a key role in stabilizing the myoplasm during contraction and relaxation. IFs also influence cell shape and motility, anchor cell structural components, support nuclear architecture, and modulate the propagation of signals within cells [10–13]. The major IF proteins of mature striated muscle are the nuclear lamins, desmin, several keratin subunits, including K8, K18 and K19, and synemin [14–16]. Here we focus on synemin and its role in the heart.

Synemin is a large IF protein that can be expressed in one of two isoforms, α (~210 kDa), and β (~180 kDa) [17,18]. Unlike desmin, and keratins 8 and 18, and 8 and 19, synemin is incapable of forming stable IFs on its own and thus requires other IF proteins to form heterofilaments [19]. In neonatal cardiomyocytes, α-synemin stabilizes junctional complexes at the sarcolemma, whereas β-synemin appears to mediate the association of desmin with Z-disks [20]. In addition to desmin, synemin can associate with vimentin in developing heart muscle [19,21]. Synemin is also an A-kinase anchoring protein (AKAP) involved in regulating the phosphorylation of proteins at the sarcolemma and Z-disks via protein kinase A [22,23]. In its role as an AKAP, synemin may regulate the activities of key signaling cascades in the heart, such as those controlled by Akt, PKA RII, and MAPKs such as ERK 1/2 [23,24].

We have studied mice lacking synemin to determine the consequences of its absence on the structure and function of mature cardiac muscle. Our findings suggest that, although

the organization of the myoplasm is not altered in the absence of synemin, cardiac muscle lacking synemin shows a mixed hypertrophic and dilated cardiomyopathic phenotype, with features of left ventricular (LV) systolic dysfunction as early as 3 months old, and LV hypertrophy and dilatation at older ages (12–16 mo old). Year-old synemin-null mice also show an increase of ~30% in the total body weight. Defects linked to the absence of synemin are endogenous to cardiomyocytes, as both Ca^{2+} transients and contractile shortening are altered in cells isolated from the synemin-null heart, compared to controls. The absence of synemin also alters the levels of several proteins in signaling pathways that have been associated with cardiomyopathy. Our results suggest that synemin is essential for cardiac health.

2. Materials and methods

2.1. Animals

Synemin-null (synm −/−) animals were generated by inserting cDNA encoding β-galactosidase into the synemin gene by homologous recombination and have been described elsewhere [25]. We used synm −/− mice at young (3 mo) and old ages (12–16 mo) and age-matched male C57Bl/6 controls (WT) for all studies reported here. Animals subjected to closed chest catheterization were anesthetized with 2.5% isoflurane inhalation (VetEquip, Pleasanton, CA) with oxygen at 0.8 l/min at 14.7 Psi (21 °C) and then euthanized by cervical dislocation. All of our protocols were approved by the Institutional Animal Care Committee of the University of Maryland School of Medicine.

2.2. Echocardiography

Transthoracic M-mode echocardiography using high-resolution ultrasound biomicroscopy was performed using the Vevo 2100 imaging system (Fiji-VisualSonics, Toronto, ON, Canada) equipped with a 40-MHz scanhead. Images of the LV in the parasternal short-axis view were obtained at the level of the papillary muscles under light anesthesia (inhalation of 1.2–1.5% isoflurane in oxygen). A core temperature of 37.5 °C was maintained during the measurement via a thermoregulated platform (THM 150, Indus Instruments, Houston, TX). Data were calculated according to generally accepted formulae, as we have used previously [26].

2.3. Left ventricular pressure-volume (PV) loop analysis

Under 2–2.5% of isoflurane inhalation, animals were orally intubated and ventilated via a rodent ventilator (Model 683, Harvard Instruments, Holliston, MA), at a tidal volume of 10–12 ml/kg BW with a ventilatory rate of 60–100 breaths/min. The right carotid artery was cannulated with a conductance catheter (1.2 French, Transonic-Science, London, ON, Canada), and its tip was positioned into the LV. A P10 silicone tube was cannulated into the left jugular vein for administration of 0.9% sodium chloride (0.1 ml/g BW/h). Midline laparotomy was performed, and the inferior vena cava (IVC) was visualized at the level of the origin of the right renal vein after the abdominal tissues were gently retracted with 37 °C wet (0.9% sodium chloride) gauze. A 4–0 silk suture was placed around the IVC and exteriorized through the abdominal wound. The wound was covered with the warm wet gauze. After 10–15 min stabilization under 1.5% isoflurane, the loop data were recorded via

the ADVantage System (ADV500, Transonic-Science), prior to and during temporary IVC occlusion created by pulling of the IVC suture for approximately 10 s. The IVC occlusion was repeated 3 times at intervals of at least 5 min. Following PV loop recordings, the catheter tip was repositioned to the aorta for blood pressure (BP) recordings. The data were analyzed offline with LabChart Pro (Version 8.1.5, ADInstruments, Sydney, Australia). All the indices were defined according to generally accepted formulae [27].

2.4. Contractile and calcium measurements

Ventricular myocytes were enzymatically isolated from WT and synm −/− mice as previously described [28]. Myocytes were maintained in Tyrode's solution (in mM: 140 NaCl, 5.4 KCl, 0.5 $MgCl_2$, 0.33 NaH_2PO_4, 11 glucose, 5 HEPES, and 1.8 $CaCl_2$, pH 7.4), at room temperature and used for experiments up to 4 h after dissociation. Prior to experiments, myocytes were loaded with 5 μM Indo-1 AM (TEFLABS Inc., Austin, TX) for 30 min at room temperature. Myocytes were then washed to remove extracellular dye and left for 30 min for de-esterification. Afterwards, myocytes were placed in a custom imaging chamber on an inverted microscope equipped with a dual PMT fluorescence system (Ionoptix), Sutter DG-4 excitation source, and a high-speed sarcomere length camera system (Aurora), all controlled by Fluorotrack software (Aurora, ON, Canada). Unloaded myocytes were paced at 1 Hz (2 ms, square pulses, 40 V) to elicit contractions while simultaneous measures of sarcomere length (SL) and Indo-1 fluorescent transients were collected.

2.5. Hematoxylin and eosin staining

Frozen cross sections, 5–8 μm thick, were fixed with cold acetone, air dried, immersed in Harris hematoxylin (Sigma-Aldrich, St. Louis, MO) for 5 min, then in Scotts Bluing reagent (ThermoFisher Scientific) for 1 min, followed by 10 rapid dips in Wright Eosin staining, with rinsing steps of tap water between solution changes, and finally through a gradient of increasing concentrations of ethanol, as previously described [25]. Coverslips were mounted with Permount (ThermoFisher Scientific). The sections were observed under light microscopy (Zeiss Axioscope, × 20 objective and × 2 eyepiece), and representative digital images were captured.

2.6. Masson trichrome staining

Frozen cross sections of 5–8 μm were fixed with cold acetone, air dried, immersed in Bouin's solution for 20 min at 56 °C, then in Weigert's Iron Hematoxylin for 7 min. Additional staining was with Biebrich Scarlet-Acid Fuchsin for 6 min, phosphotungstic/phosphomolybdic acid for 3 min, and then with Aniline Blue for 2 min. All solutions were from Sigma-Aldrich and each was followed by rinsing in tap water. Samples were then exposed to 1% acetic acid for 1 min, put through a gradient of increasing concentrations of ethanol, and finally washed with xylene. Coverslips were mounted in Permount and visualized by light microscopy, as above.

2.7. Immunofluorescence labeling

Frozen heart muscles were cryosectioned in 5–8 μm slices, fixed with cold 4% paraformaldehyde for 5 min, washed with PBS, permeabilized with Triton X-100 in

PBS (1% w/v) for 15 min, washed with PBS and incubated overnight in Superblock (ThermoFisher Scientific) before incubation with antibodies. Chicken antibodies were against βI-spectrin (1:100) [29]; rabbit antibodies were to synemin (1:20) [25] and cardiac myosin (1:00, Abcam, Cambridge, MA), dystrophin and desmin (1:100, ThermoFisher Scientific, Waltham, MA); mouse antibodies were to obscurin (1:50) [30], and alpha-actinin (1:200; Sigma-Aldrich). Fluorescent phalloidin (1:200) was from Molecular Probes (Eugene, OR). Species-specific secondary antibodies coupled to Alexa Fluor 488 or Alexa Fluor 568 were from Molecular Probes/ThermoFisher Scientific. Samples were observed under confocal optics (LSM 510 Carl Zeiss, Oberkochen, Germany) with a × 40/NA 1.4 objective with the pinhole set from 85 to 100 and the Airy unit < 1. The relative size of cardiomyocytes was determined measuring the minimal Feret's diameter [25,31] with a digital caliper, from nine randomly selected visual fields per heart, from images of frozen cross sections labeled with antibodies to dystrophin. Three hearts per group were analyzed.

2.8. Western blotting

Hearts from synm-null and control mice were dissected, followed by a slow freezing process, consisting of immersion in isopentane at −160 °C, then in liquid N_2; samples were stored at −80 °C. Muscles were homogenized in cold lysis buffer using a TissueLyser (Qiagen, Germany). Lysis buffer consisted of Mammalian Protein Extraction Reagent (Pierce, Rockford, IL), 300 mM NaCl, 40 mM EDTA, 10 mM PBS, and 10 μg/ml protease inhibitor cocktail (Sigma-Aldrich). Lysates were subjected to centrifugation. The supernatant was boiled in SDS-PAGE sample buffer for 5 min and separated by SDS-PAGE on 4–15% gradient acrylamide gels (Bio-Rad, Hercules, CA). Proteins were electrophoretically transferred at 4 °C to a nitrocellulose membrane (Invitrogen, Carlsbad, CA) at 15 V overnight. The membrane was incubated with “blocking buffer” (0.1% Tween-20, 5% BSA in Tris-buffered saline (TBS) pH 7.4), then incubated with primary antibodies in the same buffer overnight, washed with TBS plus 0.1% Tween-20 and incubated on secondary antibodies diluted in blocking buffer for 1 h. After a 30 min wash, bands were visualized by chemiluminescence (Super Signal Chemiluminiscent Substrate; ThermoFisher Scientific).

We used rabbit antibodies to study signaling proteins in the extracts: to PKA-RII (1:1000) and to the phosphopeptide containing phospho-Ser 96 of PKA-RII (1:100, Millipore, Billerica, MA); to AKT and the peptide containing phospho-Ser 473 of AKT (both at 1:10,000; Cell Signaling Technology, Danvers, MA); to ERK1/2 and the peptide containing phospho-Thr 202 and phospho-Tyr 204 of ERK1/2 (both at 1:1000, Cell Signaling Technology); to 70S6K and the peptide containing phosphoThr 38 of 70S6K (both at 1:1000, Cell Signaling Technology); and to CREB and the peptide containing phospho-Ser 133 of CREB (both at 1:250, Upstate Biotechnology, Lake Placid, NY). Rabbit antibodies to desmin (1:10,000, ThermoFisher Scientific); and mouse antibodies to GAPDH (1:20,000, Ambion, Austin, TX) were used as loading controls. Horseradish peroxidase (HRP)-conjugated anti-rabbit IgG or anti-mouse IgG (1:10,000, KPL, Gaithersburg, MD) was used to visualize all bound antibodies. The blots were quantified with Image J software (NIH, Bethesda, MD). Results are presented as a ratio of the labeling of the antibodies

to each phosphopeptide compared to the total labeling of each protein, and normalized to GAPDH.

2.9. Statistics

All values are reported as mean ± SD with $P < 0.05$ considered statistically significant. Statistical significance was accessed with the paired Student's *t*-test, 1-way ANOVA for experiments done at the same age and the unpaired t-test and 2-way ANOVA with a Tukey post-hoc analysis for studies of the same genotype. For comparison of fiber diameters, we used Fisher's exact test χ^2, 2-determinants.

3. Results

We studied the hearts of synm −/− mice in vivo and cardiomyocytes in vitro to assess the role of synemin in the structure and function of cardiac muscle in mice at young and older ages.

3.1. Echocardiographic data

We used echocardiography as a non-invasive method to evaluate changes of LV geometry and function in WT and synm −/− mice at young and older ages. The old (12 months) synm −/− hearts had greater LVDs (Fig. 1A, $p < 0.05$), which is likely consequent to reduced contractility, because LVDd (Fig. 1B) was not significantly different between the two groups. The young (3 months) synm-null hearts had significantly lower LVFS (Fig. 1C $p < 0.05$) and LVEF (Fig.1D, $p < 0.05$), both indices associated with decreased LV contractility compared to young WT mice. The young synm −/− showed a significantly lower LV posterior wall thickness (LVPWs and LVPWd, Table A.1, $p < 0.05$ for both); calculated LV mass was not significantly different from the controls of the same age, however (Fig. 2E). Compared to the old WT mice, the old synm −/− also had significantly lower LVFS and LVEF (Fig. 1C, D, $p < 0.05$ both) and greater LVDs (Fig. 1A, $p < 0.05$). Unlike the young synm −/− mice, the old synm-null mice also demonstrated a greater LVDd compared to the old WT (Fig. 1B, $p < 0.05$), indicating LV dilation, and greater LV mass (Fig. 1E, $p < 0.05$), which suggests LV myocardial hypertrophy.

The hearts of old synm −/− mice showed a significantly greater LVDs, LVDd, LVFS, LVEF, LV mass (Fig. 1A–E, $p < 0.05$ for all) and heart rate (Table A.1, $p < 0.05$) compared to young synm −/−. Comparing the young and old WT, the latter had a significantly greater LVDd, LVFS, LVEF (Fig. 1B–D, $p < 0.05$), but lower LV mass (Fig. 1E, $p < 0.05$) and E/A ratio (Table A.1, $p < 0.05$).

LV M-mode images from one animal of each group is represented in Fig. 1F–I. Relative to the two WT mice, LV posterior wall was visually more flattened in the two synm −/− mice, which suggests a reduced fractional shortening during cardiac cycles.

In summary, echocardiography suggests that both young and old synm −/− showed reduced LV contractility, but only the old synm −/− had LV dilatation and hypertrophy.

3.2. LV pressure-volume loop analysis

We next performed PV loop analysis to evaluate LV performance, as it is less confounded by loading conditions than echocardiography [27,32]. Our results were summarized in Fig. 2A–J and in Table A.1.

Compared to 3-mo WT, the synm −/− mice at the same age had a significantly higher LVEDP (Table A.1, $p < 0.05$), which indicates increases in LV preload, and significantly lower values of those indices associated with LV systolic function, including LVEF (Table A.1), +dP/dt, Ees, PRSW, and +dP/dt-EDP (Fig. 2C, D, E, F respectively, $p < 0.05$). The last three indices were obtained under temporary occlusion of the inferior vena cava, which is considered as more "loading-independent" and therefore more specific for evaluation of LV systolic function (i.e. "contractility") [27,32]. These results are consistent with our echocardiographic findings that LVEF and LVFS were reduced in young synm −/− heart.

The young synm −/− mice showed no significant changes in any other LV indices compared to the young WT, including global (HR, SV, and CO), LV diastolic (Tau, −dP/dt, and EDPVR) and vascular indices (MAP and Ea) (See Table A.1).

The old synm −/− mice showed significant increments in LVEDP (Table A.1, $p < 0.05$), and significant decrements in Ees, PRSW, +dP/dt-EDP (Fig. 2 D,E,F, $p < 0.05$), and LVEF (Table A.1) compared to old WT. Unlike the young synm −/−, the old null mice further demonstrated significant decreases in those indices associated with LV global performance, including SV, CO, and their normalized values by body weight, and SW (Fig. 2A, B, Table A.1, $p < 0.05$). Except for a significant decrease in −dP/dt, the old synm −/− mice showed no significant changes in other diastolic functional indices, Tau and EDPVR, nor any changes in MBP and Ea, compared to WT of the same age (Table A.1).

Compared to young WT mice, the old WT showed a significantly greater CO, and significantly smaller CO/BW, +dP/dt, and Ea (Table A.1, $p < 0.05$). The old synm −/− mice had a significantly lower +dP/dt, PRSW, +dP/dt-MAP, CO, CO/BW, SV/BW, SW, LVEF (Fig. 2A–F, Table A.1, $p < 0.05$) than the young synm −/− mice, suggesting a further deterioration of LV systolic function with age.

In summary, PV loop studies indicate that the LV systolic function (i.e., contractility) is compromised in synm-null hearts at both ages, and that more extensive deficits in cardiac function and global performance are apparent in the old synm-null mice.

3.3. Contractile and calcium measurements

The results obtained from cardiac catheterization and echocardiographic studies suggested a decrease in cardiac contractility. To address whether this effect was intrinsic to the cardiomyocyte, we examined contractility and Ca^{2+} signaling in single cardiomyocytes isolated from young and old mice that contracted under no-load conditions.

In response to contractions elicited by action potentials under no-load conditions, synm-null cardiomyocytes showed a significant decrease in the magnitude of sarcomeric shortening compared to WT myocytes (3 mo old: 5.7%* and 7.6%* respectively; 12 mo old: 5.6%* and

8.1%*, respectively, *p < 0.05; Fig. 3A, G). They also showed a significant decrease in the rate of shortening for both young and old synm −/− cells (Fig. 3B, H, p < 0.05) though not in the rate of relaxation (Fig. 3C, I). While alterations in contractility occurred independent of any alterations in Ca^{2+} handling in cardiomyocytes from young null mice, a decrease in the Ca^{2+} transient amplitude was identified in cardiomyocytes from the old synm −/− mice. Given the identified deficits in young and old synm-null cardiomyocytes, we conclude that the impact of the absence of synemin leads to changes that are at least in part intrinsic to the cardiomyocyte.

3.4. Morphology of old synemin–null hearts

Our identification of age-related functional alterations in the synm-null hearts led us to examine them for morphologic changes. We identified a significant increase in the mass of the old synm-null hearts (31% vs. control, p < 0.05) and observed obvious signs of ventricular hypertrophy (Fig. 4A, B), increased body weight (Fig. 4C) and characteristic patterns of hypertrophic CM compared to controls (Fig. 4D, E).

We next used histochemical and immunofluorescence methods to examine the morphology of the hearts from year-old mice to learn if the absence of synemin affects muscle structure at the tissue and cellular levels (see Fig. 5, A–F and I–J). Cross sections of frozen synm −/− hearts revealed a modest hypertrophy including a slightly higher number of nuclei (increase of 20%; p < 0.05; Fig. 5A and D; quantitated in Fig. 5G), a small increase in fibrosis (Fig. 5B, E), and modest enlargement of cardiomyocytes, as indicated by an increase in the mean minimal Feret's diameter (11%; p < 0.05; Fig. 5C, F) compared to controls (quantitated in Fig. 5H).

We confirmed that synemin was absent from the myocytes in synm-null mice by immunofluorescence (Fig. 5I, J). Labeling of cross sections of WT heart showed the characteristic reticular structure containing synemin that surrounds the myofibrils within the interior of each fiber (Fig. 5I, insert). Synemin was also present at the sarcolemma, where dystrophin was also concentrated. Synemin within and at the periphery of cardiac myocytes was completely absent in cross sections of synm-null heart (Fig. 5J).

We further examined longitudinal cryosections of heart muscles from control (Fig. 6A–D and I–K) and synm-null mice (Fig. 6E–H and L–N) to learn if the organization of the contractile apparatus and of costameres was altered. The absence of synemin does not alter the organization of either sarcolemmal or costameric proteins in heart. The organization of M-bands, visualized with antibodies to obscurin, was unaffected in synm −/− myocytes (Fig. 6A, E). IF structures at the level of Z disks, labeled with anti-desmin and anti-α-actinin, also appeared to be unaffected (Fig. 6 B,F and I,L). Additional studies with antibodies to cardiac myosin heavy chain (Fig. 6 J,M) and with fluorescein-phalloidin (Fig. 6 K,N), failed to show changes in the organization of A bands or I-bands, respectively. Similarly, β-spectrin at costameres was not significantly altered by the absence of synemin (Fig. 6 C,G). This is in keeping with our observations of sections of heart labeled with anti-dystrophin (Fig. 5 C,F). These results suggest that synemin is not required for the normal architecture of the sarcomeres or costameres in old murine heart muscle (Fig. 6 D,H).

3.5. Western blot analysis of signaling proteins

We prepared immunoblots of synm −/− and WT heart muscle and probed them with antibodies to several signaling proteins and their phosphorylated derivatives that are known to be active in the heart (Fig. 7A). The phosphorylated levels of the regulatory subunit II of protein kinase A (PKARII (Ser96)) (Fig. 7B) and the phosphorylated form of ERK 1/2 (Thr202/Tyr204) (Fig. 7C), each decreased relative to unphosphorylated protein in synm-null heart compared to WT. By contrast, the phosphorylation of the ribosomal protein, 70S6K (Thr389) relative to unphosphorylated 70S6K increased in the synm −/− tissue (Fig. 7D). By contrast, the relative amounts of the phosphorylated forms of AKT and CREB did not vary significantly between synm-null and WT hearts (Fig. 7E,F). Desmin protein expression levels were also the same (Fig. 7G), consistent with the results shown in Fig. 6B,F.

4. Discussion

Intermediate filaments (IFs) are associated with the contractile apparatus and the sarcolemma in striated muscle and play important roles in resistance to mechanical stress, force transduction, targeting of proteins and lipids, and regulation of key signaling pathways [10,11,15,33]. Although the major IF protein in mature striated myocytes is desmin, synemin and keratins are also abundant in mature muscle tissue [15,24,34]. Unlike desmin and the keratins, synemin is a large IF protein that can be expressed in two isoforms, α and β, and requires other IF proteins such as desmin to form heterofilaments [19]. We and others have previously reported that the absence of synemin in murine skeletal muscle is associated with a modest myopathy [25,35]. We also recently showed that the absence of synemin causes osteopenia in skeletal tissue [36]. Here we examine the heart, which like skeletal muscle and bone is of mesenchymal origin, and demonstrate that the absence of synemin in mice elicits some features of a mixed hypertrophic and dilated cardiomyopathy associated with significant changes in cardiac function. Our results support the conclusion that synemin plays an important role in the heart.

Although our study is the first to show altered cardiac function related to the absence of synemin, cardiomyopathies (CM) have previously been linked to other IF proteins. Dilated CM, arrhythmogenic right ventricular CM and mixed CM with arrhythmia are associated with abnormalities in proteins of the IF superfamily, such as desmin, lamin A and lamin C [37–44]. Concentric hypertrophy, cardiac dilation with compromised systolic function due to fibrosis, calcification, lateral misalignment of myofibrils, changes in the dimensions of individual cardiomyocytes, as well as decreases in active force generation, have been reported in desmin-null mice [38,44–46]. Increases in both desmin and vimentin have been reported in cardiac biopsies of patients with dilated CM [44]. Vimentin has been proposed to be an early diagnostic of myocardial sclerosis, due to its intense appearance in the interstitial tissue of diseased ventricular myocardium [47].

It is notable that heart rate during echocardiography was significantly higher in older than in younger synm −/− mice. We did not find this difference in our PV loop study, likely because of confounding effects of the deeper initial anesthesia, mechanical ventilation and thoracotomy. Although further study will be needed to determine the significance of the

change in heart rate, it may be linked to sympathetic hyperactivity associated with LV dysfunction and aging [48].

There is significant depression in LV in vivo systolic function in both young and old synm −/− hearts, documented by echocardiographic indices (LVEF and LVFS) and the "loading-independent" indices from PV loop analysis (Ees, PRSW, and +dP/dt-EDP), while LV afterload appears normal (no changes in MBP and Ea). Like desmin-null mice, the present study suggests that mice lacking synemin show features of both hypertrophic and dilated CMs as they reach 1 year of age. Additionally, old mice also show LV hypertrophy, indicated by increases in LV mass (echocardiography), cardiomyocyte size, and heart weight, as well as LV dilatation that is indicated by increases in LVDd (echocardiography). It is interesting that the young synm −/− heart presents marked LV systolic dysfunction but lacks LV hypertrophy and dilatation. Further study in neonatal or juvenile mice would further determine if the systolic dysfunction observed is truly an age-independent change.

Increments in myocyte size, in left ventricular mass and in diastolic pressure (reduced blood supply), a higher number of nuclei and an increase in fiber diameter are characteristic of hypertrophic disease. By contrast, an absence of changes in wall thickness, coupled with increases in LV diastolic and systolic volumes and systolic pressure, and decreases in LV ejection fraction and fractional shortening, together with cardiac remodeling, are indicative of dilated CM. Defects in many proteins, including proteins that regulate the organization and function of the sarcomere and sarcolemma, like myosin and desmin, have been linked to both types of cardiomyopathy. Defects in cellular signaling mechanisms also lead to hypertrophic cardiomyopathy [49–53]. As synemin is a structural protein associated with both sarcomeres and sarcolemma, and an AKAP that can indirectly regulate the phosphorylation state of nearby proteins [21,23,54], it is not surprising that its absence can lead to a mixed phenotype.

Although it is only one of 18 different AKAPs in the heart, synemin's AKAP activity and its absence in the synm-null heart may be responsible for the changes in the levels of signaling molecules reported earlier in skeletal muscle [24] and here in the heart. In particular, we find that the relative levels of phosphorylated PKAR II, 70s6K and ERK1/2 change to small but significant extents in the whole synemin-null heart. Of these, PKARII and pERK1/2 are likely to be the most significant. PKA can be activated by a number of hormones and growth factors and can lead to physiologically significant changes in cardiac function through its ability to phosphorylate phospholamban and several contractile proteins [50]. ERK1/2, which can phosphorylate over 100 possible substrates, has also been linked to cardiovascular disease [54,55] and is likely to contribute to hypertrophy in the myocardium ([56–59], but see [60]), consistent with our finding of a change in pERK1/2 levels in the myopathic synm −/− heart. Thus, our finding that PKARII and pERK1/2 are altered in synm-null hearts provides a possible molecular pathway underlying the cardiomyopathy we have characterized.

Our identification of deficits in contractility and Ca^{2+} signaling in synm-null cardiomyocytes (Fig. 3) is consistent with the decreased contractility and impaired ejection fraction in the heart. Within the cardiomyocytes, synemin is associated with both costameres

(α-synemin) and with the intermediate filament system surrounding the contractile apparatus at Z-disks (β-synemin) [20]. While its absence in the heart [61], skeletal tissue [36] or skeletal muscle [25] does not result in obvious structural alterations as detected by immunolabeling and confocal microscopy, its absence in bone results in the loss of trabecular and cortical bone related to defective osteoblast production [36], and measures of elastimetry [25] in skeletal muscle suggest that biomechanical deficits arise in synemin's absence, driven either by rearrangements of the protein complexes associated with the sarcolemma and sarcomere, or by changes in signaling. Based on this new evidence that synemin is involved in the function of the cardiomyocyte, our future studies will seek to define its biomechanical and regulatory roles in cardiac muscle.

5. Conclusion

Although the mechanisms remain to be discovered, our results show that synemin plays a physiologically significant role in cardiac muscle, and its absence leads to changes in structure and function associated with cardiomyopathy.

Supplementary Material

Refer to Web version on PubMed Central for supplementary material.

Acknowledgments

We thank Andrea O'Neill for assistance with immunolabeling and figure preparation. Our research has been supported in part by a Physiological Genomics Fellowship-APS and UNAM-PAPIIT (IA 209016) to KPGP, by a CNPq/CAPES-Science without Borders Scholarship to HCJ, by a donation from the Kahlert Foundation and by grants from the National Institutes of Health to CWW (R01 AR062554), WJL (R01 HL105239, U01 HL116321), and RJB (R01 AR 055928).

Abbreviations

+ dP/dt	maximal rate of left ventricular pressure rise
−dP/dt	maximal rate of left ventricular pressure fall
+ dP/dt-EDP	end-diastolic pressure adjusted maximal rate of left ventricular pressure rise
AKAP	A-kinase anchoring protein
AKT	protein kinase B also known as Akt
BP	blood pressure
BW	body weight
CM	cardiomyopathy
CO	cardiac output
CREB	cAMP response element-binding protein

DCM	dilated cardiomyopathy
E/A	the ratio of the early (E) to late (A) filling velocities of the left ventricle
ECM	extracellular matrix
EDP	end-diastolic pressure
EDPVR	the slope of the end-diastolic pressure-volume relationship
EF	ejection fraction
ERK 1/2	extracellular signal-regulated kinase 1/2
ESP	end-systolic pressure
Ea	effective arterial elastance
Ees	the slope of left ventricular end-systolic pressure-volume relationship
FS	fractional shortening
HCM	hypertrophic cardiomyopathy
HR	heart rate
IFs	intermediate filaments
IVC	inferior vena cava
LV	left ventricle or left ventricular
LVDd	LV end-diastolic dimension
LVDs	LV end-systolic dimension
MAPKs	mitogen-activated protein kinases
MBP	mean blood pressure
PV	Pressure-volume
PKA RII	protein kinase A subunit II
PRSW	preload recruitable stroke work
Pes	pressure end-systolic
SL	sarcomere length
SV	stroke volume
SW	stroke work
synm −/−	synemin-null

Tau	isovolumic relaxation time constant
WT	wild type mice

References

1. World Health Organization. Cardiovascular diseases (CVDs) Fact sheet. 317 2015;
2. CDC. NCHS. Underlying Cause of Death 1999–2013 on CDC WONDER Online Database, released 2015. Data are from the Multiple Cause of Death Files, 1999–2013, as compiled from data provided by the 57 vital statistics jurisdictions through the Vital Statistics Cooperative Program. Accessed May 15, 2016
3. Walsh, R, Fang, J, Fuster, V, O'Rourke, R. Hurst's the Heart Manual of Cardiology. 13. Mc Graw Hill Education/Medical; 2012.
4. Kamisago M, Sharma S, De Palma S, Solomon S, Sharma P, McDonough B, Smoot L, Mullen M, Woolf P, Wigle D, Seidman J, Seidman C. Mutations in sarcomere protein genes as a cause of dilated cardiomyopathy. The New England J. Med. 343 (23) 2000; :1688–1696. [PubMed: 11106718]
5. Hershberger, R; Morales, A. Dilated cardiomyopathy overview. Gene Reviews [Internet]. 2015. Retrieved January 03, 2016 from http:www.ncbi.nlm.nih.gov/books/NBK1309
6. Maron B. Hypertrophic cardiomyopathy. Circulation. 106 2002; :2419–2421. [PubMed: 12417536]
7. Wang L, Seidman J, Seidman C. Harnessing molecular genetics for the diagnosis and management of hypertrophic cardiomyopathy. Ann. Intern. Med. 152 (8) 2010; :513–W181. [PubMed: 20404382]
8. Tian T, Liu Y, Zhou X, Song L. Progress in the molecular genetics of hypertrophic cardiomyopathy: a mini-review. Gerontology. 59 (3) 2013; :199–205. [PubMed: 23363806]
9. Ashrafian H, McKenna W, Watkins H. Disease pathways and novel therapeutic targets in hypertrophic cardiomyopathy. Circ. Res. 109 2011; :86–96. [PubMed: 21700950]
10. Paramio J, Jorcano L. Beyond structure: do intermediate filaments modulate cell signaling? Bioassays. 24 (9) 2002; :836–844.
11. Kim S, Coulombe P. Intermediate filament scaffolds fulfill mechanical, organizational, and signaling functions in the cytoplasm. Genes Dev. 21 2007; :1581–1597. [PubMed: 17606637]
12. Herrmann H, Strelkov SV, Burkhard P, Aebi U. Intermediate filaments: primary determinants of cell architecture and plasticity. J. Clin. Invest. 119 2009; :1772–1783. [PubMed: 19587452]
13. Stone MR, O'Neill A, Lovering RM, Strong J, Resneck WG, Reed PW, Toivola DM, Ursitti JA, Omary MB, Bloch RJ. Absence of keratin 19 in mice causes skeletal myopathy with mitochondrial and sarcolemmal reorganization. J. Cell Sci. 120 2007; :3999–4008. [PubMed: 17971417]
14. O'Neill A, Williams MW, Resneck W, Milner D, Capetanaki Y, Bloch RJ. Sarcolemmal organization in skeletal muscle lacking desmin: evidence for cytokeratins associated with membrane skeleton at costameres. Mol. Biol. Cell. 13 2002; :2347–2359. [PubMed: 12134074]
15. Capetanaki Y, Bloch RJ, Kouloumenta A, Mavroidis M, Psarras S. Muscle intermediate filaments and their links to membranes and membranous organelles. Exp. Cell Res. 313 (10) 2007; :2063–2076. [PubMed: 17509566]
16. Omary, M, Liem, R. Intermediate Filament Proteins. Elsevier Inc.; 2016. Methods in Enzymology.
17. Becker B, Bellin RM, Sernett SW, Huiatt TW, Robson RM. Synemin contains the rod domain of intermediate filaments. Biochem. Biophys. Res. Commun. 213 1995; :796–802. [PubMed: 7654240]
18. Bilak SR, Sernett SW, Bilak MM, Bellin RM, Stromer MH, Huiatt TW, Robson RM. Properties of the novel intermediate filament protein synemin and its identification in mammalian muscle. Arch. Biochem. Biophys. 355 1998; :63–76. [PubMed: 9647668]
19. Sun N, Critchley D, Paulin D, Li Z, Robson R. Human alpha-synemin interacts directly with vinculin and metavinculin. Biochem. J. 409 2008; :657–667. [PubMed: 18028034]

20. Lund M, Kerr J, Lupinetti J, Zhang Y, Russell M, Bloch R, Bond M. Synemin isoforms differentially organize cell junctions and desmin filaments in neonatal cardiomyocytes. FASEB. 1 2011; :137–148.
21. Bellin R, Huiatt W, Critchley R, Robson M. Synemin may function to directly link muscle cell intermediate filaments to both myofibrillar Z-lines and costameres. J. Biol. Chem. 276 2001; :32330–32337. [PubMed: 11418616]
22. Sandoval IV, Colaco CA, Lazarides E. Purification of the intermediate filament-associated protein, synemin, from chicken smooth muscle. Studies on its physicochemical properties, interaction with desmin, and phosphorylation. J. Biol. Chem. 258 (4) 1983; :2568–2576. [PubMed: 6822575]
23. Russell MA, Lund LM, Haber R, McKeegan K, Cianciola N, Bond M. The intermediate filament protein, synemin, is an AKAP in the heart. Arch. Biochem. Biophys. 456 2006; :204–215. [PubMed: 16934740]
24. Pitre A, Davis N, Paul M, Orr AW, Skalli O. Synemin promotes AKT-dependent glioblastoma cell proliferation by antagonizing PP2A. Mol. Biol. Cell. 23 2012; :1243–1253. DOI: 10.1091/mbc.E11-08-0685 [PubMed: 22337773]
25. García-Pelagio K, Muriel J, O' Neill A, Desmond P, Lovering R, Lund L, Bond M, Bloch R. Myopathic changes in murine skeletal muscle lacking synemin. Am. J. Phys. Cell Phys. 308 (6) 2015; :C448–62.
26. Chen L, Zhang J, Hu X, Philipson K, Scharf S. The Na+/Ca+ exchanger-1 mediates left ventricular dysfunction in mice with chronic intermittent hypoxia. J. Appl. Physiol. 109 2010; :1675–1685. [PubMed: 20947716]
27. Pacher P, Nagayama T, Mukhopadhyay P, Bátkai S, Kass D. Measurement of cardiac function using pressure-volume conductance catheter technique in mice and rats. Nat. Protoc. 3 2008; :1422–1434. [PubMed: 18772869]
28. Shioya T. A Simple technique for isolating healthy heart cells from mouse models. J. Physiol. Sci. 57 (6) 2007; :327–335. [PubMed: 17980092]
29. Ursitti JA, Lee PC, Resneck WG, McNally MM, Bowman AL, O'Neill A, Stone MR, Bloch RJ. Cloning and characterization of cytokeratins 8 and 19 in adult rat striated muscle. Interaction with the dystrophin glycoprotein complex. J. Biol. Chem. 279 2004; :41830–41838. [PubMed: 15247274]
30. Kontrogianni-Konstantopoulos A, Jones EM, Van Rossum DB, Bloch RJ. Obscurin is a ligand for small ankyrin 1 in skeletal muscle. Mol. Biol. Cell. 14 2003; :1138–1148. [PubMed: 12631729]
31. Briguet A, Courdier-Fruh I, Foster M, Meier T, Magyar JP. Histological parameters for the quantitative assessment of muscular dystrophy in the mdx mouse. Neuromuscul. Disord. 14 2004; :675–682. [PubMed: 15351425]
32. Burkhoff D, Mirsky I, Suga H. Assessment of systolic and diastolic ventricular properties via pressure-volume analysis: a guide for clinical, translational, and basic researchers. Am. J. Physiol. Heart Circ. Physiol. 289 (2) 2005; :H501–512. [PubMed: 16014610]
33. Bloch RJ, Capetanaki Y, O'Neill A, Reed P, Williams M, Resneck W, Porter N, Ursitti J. Costameres: repeating structures at the sarcolemma of skeletal muscle. Clin. Orthop. Relat. Res. 403 2002; :S203–S210.
34. Lovering R, O' Neill A, Muriel J, Prosser B, Strong J, Bloch RJ. Physiology, structure, and susceptibility to injury of skeletal muscle in mice lacking keratin 19-based and desmin-based intermediate filaments. Am. J. Phys. 300 (4) 2011; :C803–C813.
35. Zhenlin L, Parlakian A, Coletti D, Alonso-Martin S, Hourdé C, Joanne P, Gao-Li J, Blanc J, Ferry A, Paulin D, Xue Z, Agbulut O. Synemin acts as a regulator of signaling molecules in skeletal muscle hypertrophy. J. Cell Sci. 127 2014; :4589–4601. [PubMed: 25179606]
36. Moorer M, Buo A, García-Pelagio K, Stains J, Bloch R. Deficiency of the intermediate filament synemin reduces bone mass in vivo. Am. J. Cell. Physiol. 11 (6) 2016; :C839–C845.
37. Granger BL, Lazarides E. Synemin: a new high molecular weight protein associated with desmin and vimentin filaments in muscle. Cell. 22 1980; :727–738. [PubMed: 7006832]
38. Schaper J, Froede R, Hein S, Buck A, Hashizume H, Speiser B, Friedl A, Bleese N. Impairment of the myocardial ultrastructure and changes of the cytoskeleton in dilated cardiomyopathy. Circulation. 83 1991; :504–514. [PubMed: 1991369]

39. Li D, Tapscoft T, Gonzalez O, Burch P, Quiñones M, Zoghbi W, Hill R, Bachinski L, Mann D, Roberts R. Desmin mutation responsible for idiopathic dilated cardiomyopathy. Circulation. 100 (5) 1999; :461–464. [PubMed: 10430757]
40. Brodsky G, Muntoni F, Miocic S, Sinagra G, Sewry C, Mestroni L, Lamin A. C gene mutation associated with dilated cardiomyopathy with variable skeletal muscle involvement. Circulation. 101 (5) 2000; :473–476. [PubMed: 10662742]
41. Taylor M, Fain P, Sinagra G, Robinson M, Robertson A, Carne E, DiLenarda A, Bohlmeyer T, Ferguson D, Brodsky G, Boucek M, Lascor J, Moss A, Li W, Stetler G, Muntoni F, Bristow M, Mestroni L. Natural history of dilated cardiomyopathy due to lamin A/C gene mutations. J. Am. Coll. Cardiol. 41 (5) 2003; :771–780. [PubMed: 12628721]
42. Saga A, Karibe A, Otomo J, Iwabuchi K, Takahashi T, Kanno H, Kikuchi J, Keitoku M, Shinozaki T, Shimokawa H, Lamin A. C gene mutations in familial cardiomyopathy with advanced atrioventricular block and arrhythmia. Tohoku J. Exp. Med. 218 (4) 2009; :309–316. [PubMed: 19638735]
43. Radu R, Adriana Bold, Pop O, Malaescu D, Gheorghisor I, Mogoanta L. Histological changes and immunohistochemical changes of the myocardium in dilated cardiomyopathy. Romanian J. Morphol. Embryol. 53 (2) 2012; :269–275.
44. Thornell L, Carlsson Z, Li Z, Mericskay M, Paulin D. Null mutation in the desmin gene gives rise to a cardiomyopathy. J. Mol. Cell. Cardiol. 29 (8) 1997; :2107–2124. [PubMed: 9281443]
45. Milner D, Taffet G, Wang X, Pham T, Tamura T, Hartley C, Gerdes M, Capetanaki Y. The absence of desmin leads to cardiomyocyte hypertrophy and cardiac dilation with compromised systolic function. J. Mol. Cell. Cardiol. 31 (11) 1999; :2063–2076. [PubMed: 10591032]
46. Balogh J, Merisckay M, Li Z, Paulin D, Arner A. Hearts from mice lacking desmin have a myopathy with impaired active force generation and unaltered wall compliance. Cardiovasc. Res. 53 (2) 2002; :439–450. [PubMed: 11827695]
47. Di Somma S, Marotta M, Salvatore G, Cudemo G, Cuda G, De Vivo F, Di Benedetto Ciaramella F, Caputo G, Divitiis O. Changes in myocardial cytoskeletal intermediate filaments and myocyte contractile dysfunction in dilated cardiomyopathy: an in vivo study in humans. Heart. 84 2000; :659–667. [PubMed: 11083750]
48. Toschi-Dias E, Rondon MUPB, Cogliati C, Paolocci N, Tobaldini E, Montano N. Contribution of autonomic reflexes to the hyperadrenergic state in heart failure. Front. Neurosci. 11 2017; :162. doi: 10.3389/fnins.2017.00162 [PubMed: 28424575]
49. Klauke B, Kossman S, Gaertner A, Brand K, Stork I, Brodehl A, Dieding M, Walhorn V, Anselmetti D, Gerdes D, Bohms B, Schulz U, ZuKnyphausen E, Vorgerd M, Gummert J, Milting H. De novo desmin-mutation N116S is associated with arrhythmogenic right ventricular cardiomyopathy. Hum. Mol. Genet. 19 (23) 2010; :4595–4607. [PubMed: 20829228]
50. Chung MW, Tsoutsman T, Semsarian C. Hypertrophic cardiomyopathy: from gene defect to clinical disease. Cell Res. 13 2003; :9–20. [PubMed: 12643345]
51. Ruehr ML, Russell MA, Bond M. A-kinase anchoring protein targeting of protein kinase A in the heart. J. Mol. Cell. Cardiol. 37 (3) 2004; :653–665. [PubMed: 15350838]
52. Heineke J, Molkentin J. Regulation of cardiac hypertrophy by intracellular signaling pathways. Nat. Rev. Mol. Cell Biol. 7 2006; :589–600. [PubMed: 16936699]
53. Harvey P, Leinwand L. Cellular mechanisms of cardiomyopathy. J. Cell Biol. 194 (3) 2011; :355–365. [PubMed: 21825071]
54. Diviani D, Maric D, Pérez López I, Cavin S, Del Vescovo CD. A-kinase anchoring proteins: molecular regulators of the cardiac stress response. Biochem. Biophys Acta. 1833 (4) 2013; :901–908. [PubMed: 22889610]
55. Yoon S, Seger R. The extracellular signal-regulated kinase: multiple substrates regulate diverse cellular functions. Growth Factors. 24 (1) 2006; :21–44. [PubMed: 16393692]
56. Bueno O, Molkentin J. Involvement of extracellular signal-regulated kinases ½ in cardiac hypertrophy and cell death. Circ. Res. 91 2002; :776–781. [PubMed: 12411391]
57. Chen J, Fujii K, Zhang L, Roberts T, Fu H. Raf-1 promotes cell survival by antagonizing apoptosis signal-regulating kinase 1through a MEK-ERK independent mechanism. Proc. Natl. Acad. Sci. U. S. A. 98 2001; :7783–7788. [PubMed: 11427728]

58. Flesch M, Margulies KB, Mochmann HC, Engel D, Sivasubramanian N, Mann DL. Differential regulation of mitogen-activated protein kinases in the failing human heart in response to mechanical unloading. Circulation. 104 2001; :2273–2276. [PubMed: 11696464]

59. Purcell N, Wilkins BJ, York A, Saba-El-Leil M, Meloche S, Robbins J, Molkentin J. Genetic inhibition of cardiac ERK1/2 promotes stress-induced apoptosis and heart failure but has no effect on hypertrophy in vivo. Proc. Natl. Acad. Sci. U. S. A. 104 2007; :14074–14079. [PubMed: 17709754]

60. Rose B, Force T, Wang Y. Mitogen-activated protein kinase signaling in the heart: angels versus demons in a heart-breaking tale. Physiol. Rev. 90 (4) 2010; :1507–1546. [PubMed: 20959622]

61. Garcia-Pelagio K, Chen L, Bloch R. Absence of synemin causes hypertrophy in murine heart. AIP Conf Proc. 1747 2016; doi: 10.1063/1.4954099

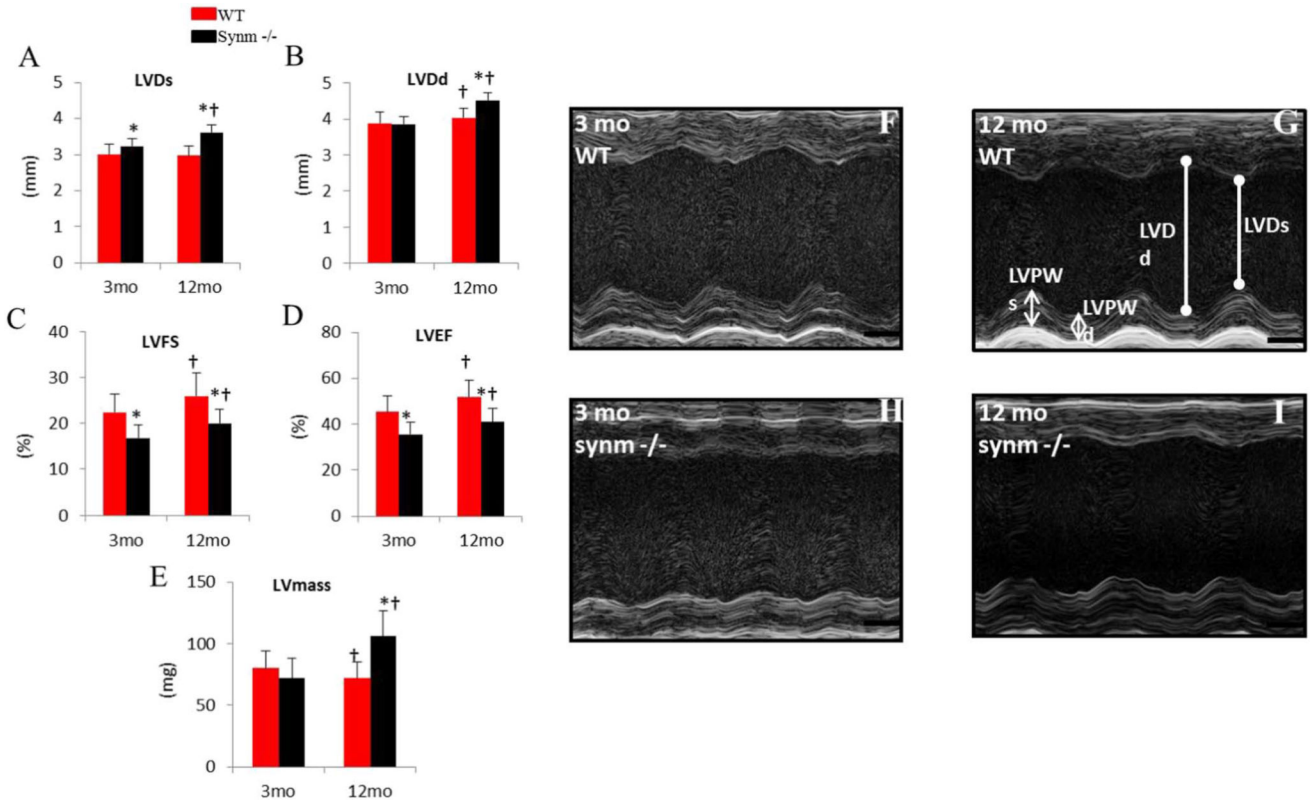

Fig. 1.

Echocardiographic results in synm-null mice at young and old ages. (A–E) Pooled data of left ventricular dimension (LVD) during systole (LVDs) (A), and diastole (LVDd) (B); LV Fractional shortening, LVFS (C); LV ejection fraction, LVEF (D); LV mass (E). (F–I) Representative M-mode images for WT and synm- null mice. n =15 at 3 mo old, and n = 7 for 12 mo old; *$p < 0.05$, compared to WT at the same age; †$p < 0.05$ compared to the 3-mo mice of the same genotype.

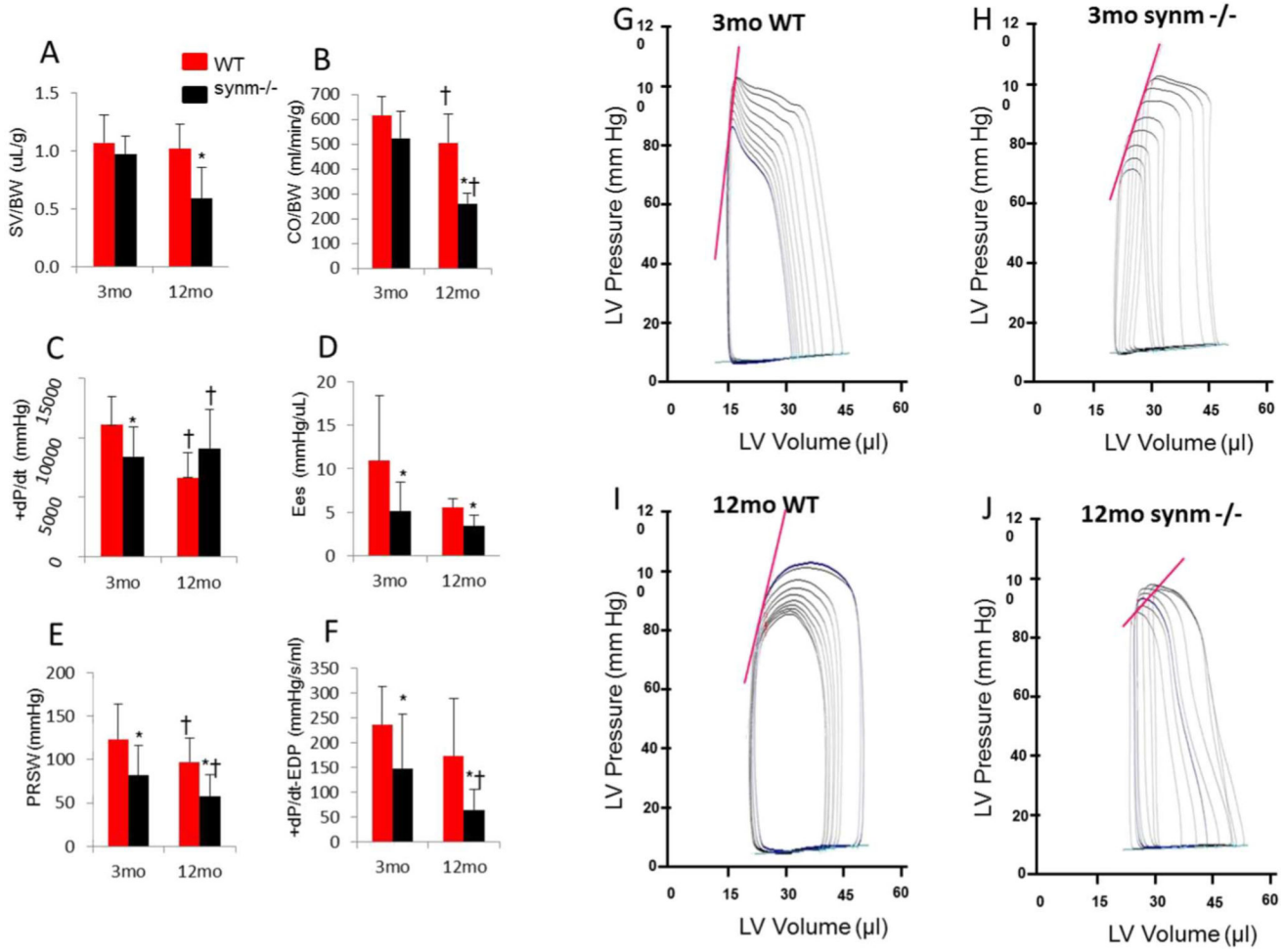

Fig. 2.

Analysis of PV loop studies. Pooled data are shown as stroke volume by body weight (SV/BW) (A); cardiac output by body weight (CO/BW) (B); maximal rate of left ventricular pressure rise (+dP/dt) (C); chamber stiffness (Ees) (D); preload-recruitable stroke work (PRSW) (E); maximum derivative of change in systolic pressure in time related to the end diastolic pressure (+dPdtmax-EDP) (F). Representative diagrams of LV pressure volume loop analysis from young WT (G), young synm −/−(H), old WT (I), and old synm −/− (J). Note that the two WT have the steeper slopes of the end-systolic PV relationship (Ees) relative to synm −/−, depicted as the straight line on the upper part of the loops, which indicates a greater LV contractility. The slopes of the end-diastolic PV relationship (EDPVR), depicted as an exponential curve on the bottom of the loops, were similar among the four animals. N=13 and 7 for young and old mice respectively. *$p < 0.05$, compared to WT of the same age; †$p < 0.05$, compared to the 3-mo mice with same genotype.

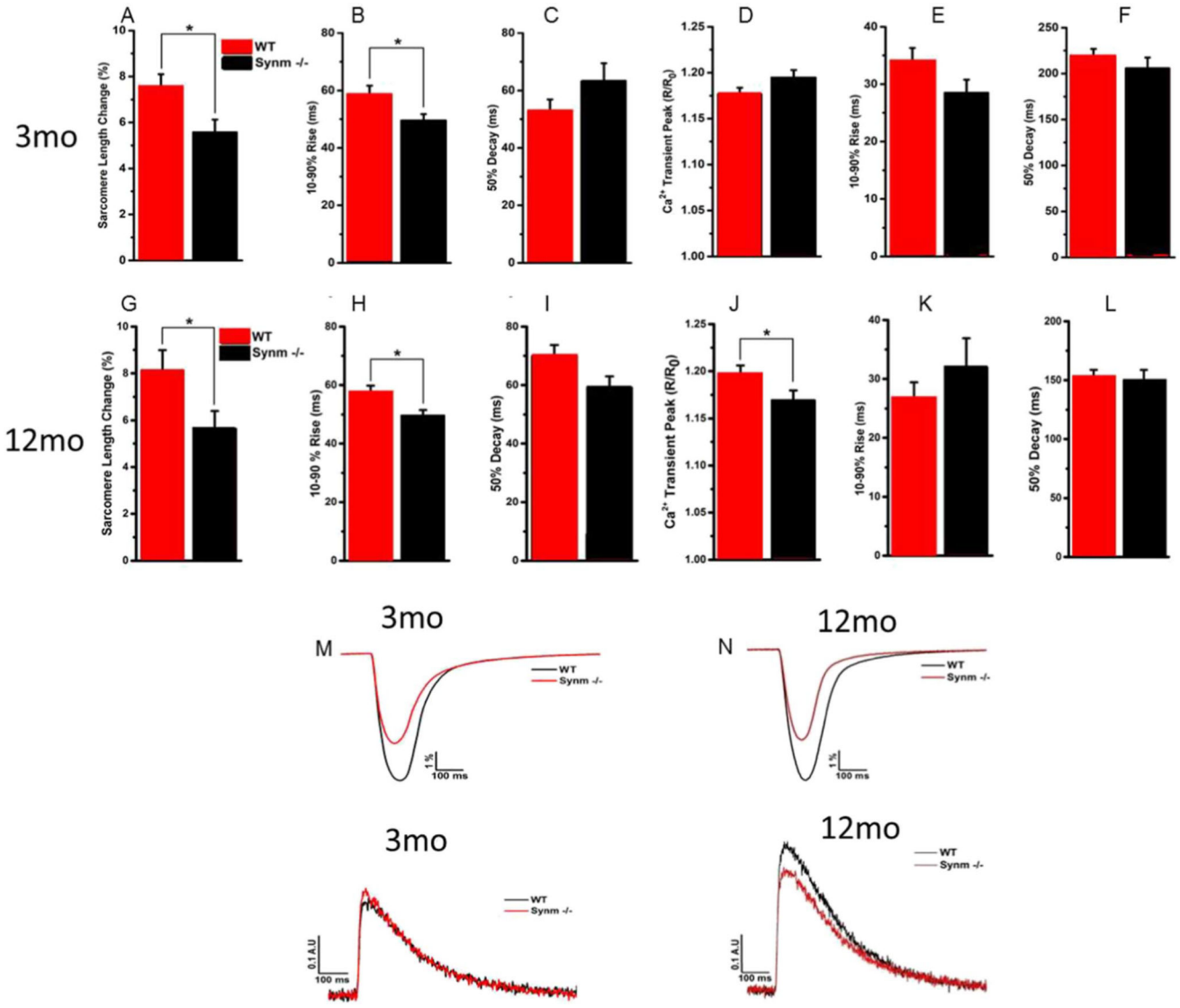

Fig. 3.

Contractility and Ca^{2+} transients in ventricular myocytes of WT and synm −/−mice at 3 and 12 mo of age. Synm −/−myocytes (n =23 and 22 cells for 3 and 12 mo old mice, respectively) showed reduced sarcomere shortening with a slightly faster contraction phase but with no changes in relaxation kinetics compared to WT cells (A–C and G–I) (n = 25 and 27 cells for 3 and 12 mo old mice, respectively; *p < 0.05). Synm −/−ventricular myocytes showed a decrease in the amplitude of the Ca^{2+} transient without changes in transient kinetics in cells from old but not young mice (D–F and J–L) (*p < 0.05). Representative traces of contractility and relaxation (upper traces) and Ca^{2+} transients (lower traces) in cardiomyocytes from young and old WT (black lines) and synm −/−(red lines) mice (M–N). (For interpretation of the references to colour in this figure legend, the reader is referred to the web version of this article.)

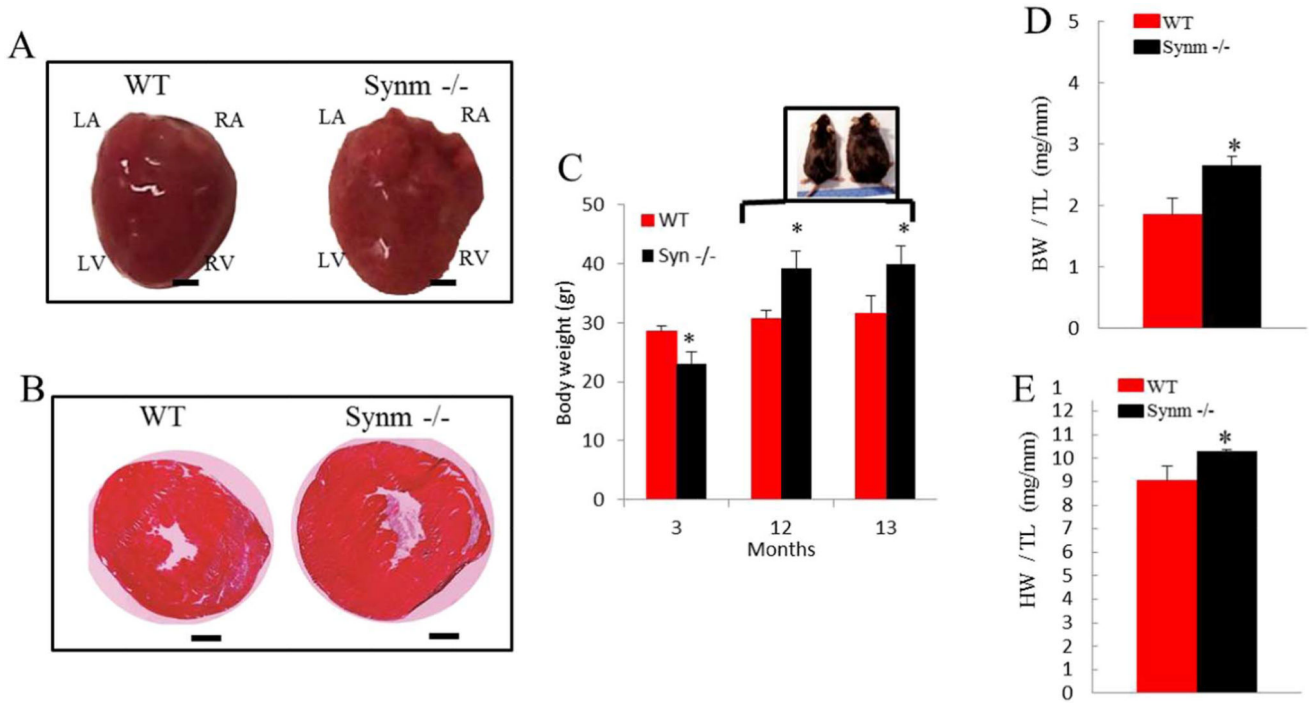

Fig. 4.

Older synm −/− mice show an increase in body weight and heart size compared to controls. Intact hearts of 13 month-old synm −/− and WT mice (A). Frozen cross sections of synm −/− and WT heart stained with hematoxylin and eosin (2×) (B). Body weight (BW) (C), and body and heart weight (HW) normalized to tibia length (TL) (D and E). *$p < 0.05$, $n = 12$; Scale bar = 1 mm.

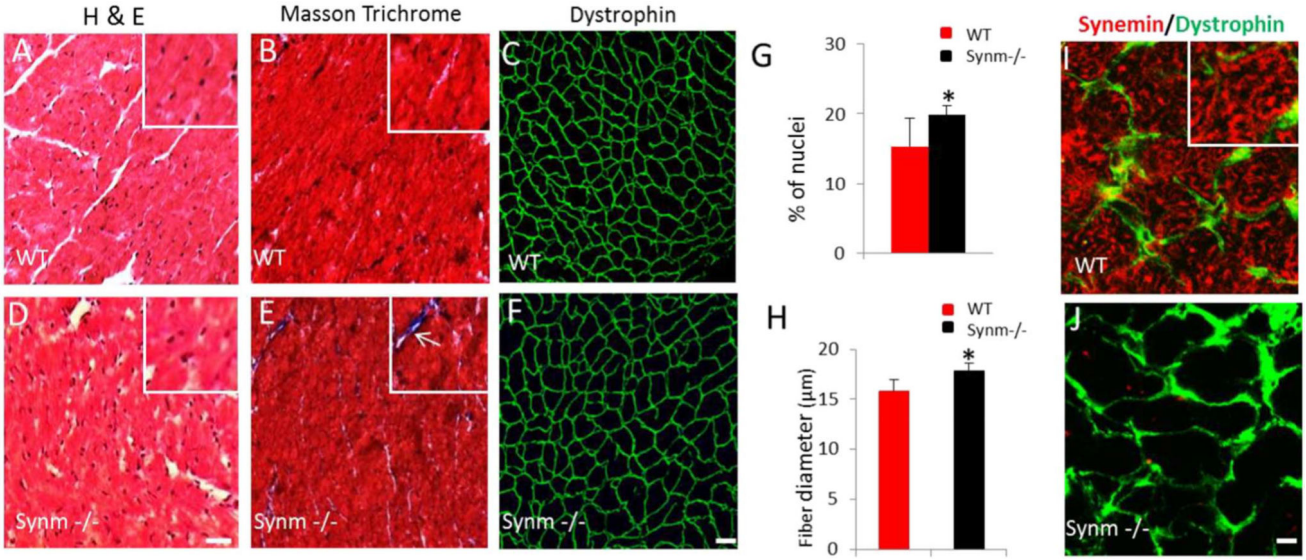

Fig. 5.

Histological changes in cardiac muscle of synm −/− and WT mice. The images show the myoplasm of cardiocytes stained with hematoxylin and eosin in pink and nuclei in blue (A,D). Masson trichrome staining revealed small regions of fibrosis (white arrow) in synm −/− heart (inset in E) (B,E). Dystrophin labeling is similar in synm −/− and controls, but the sizes of myocytes appear larger in the synm-null (C,F). Graphs show a higher number of nuclei and enlargement of cardiomyocytes in synm −/− heart (G,H). Specificity of the antisynemin antibody in cross sections of WT and synm −/− heart (I,J). *$p < 0.05$. Scale bars: C, F´= 20 µm; I,J= 5 µm. Insets are enlarged 2.5×. (For interpretation of the references to colour in this figure legend, the reader is referred to the web version of this article.)

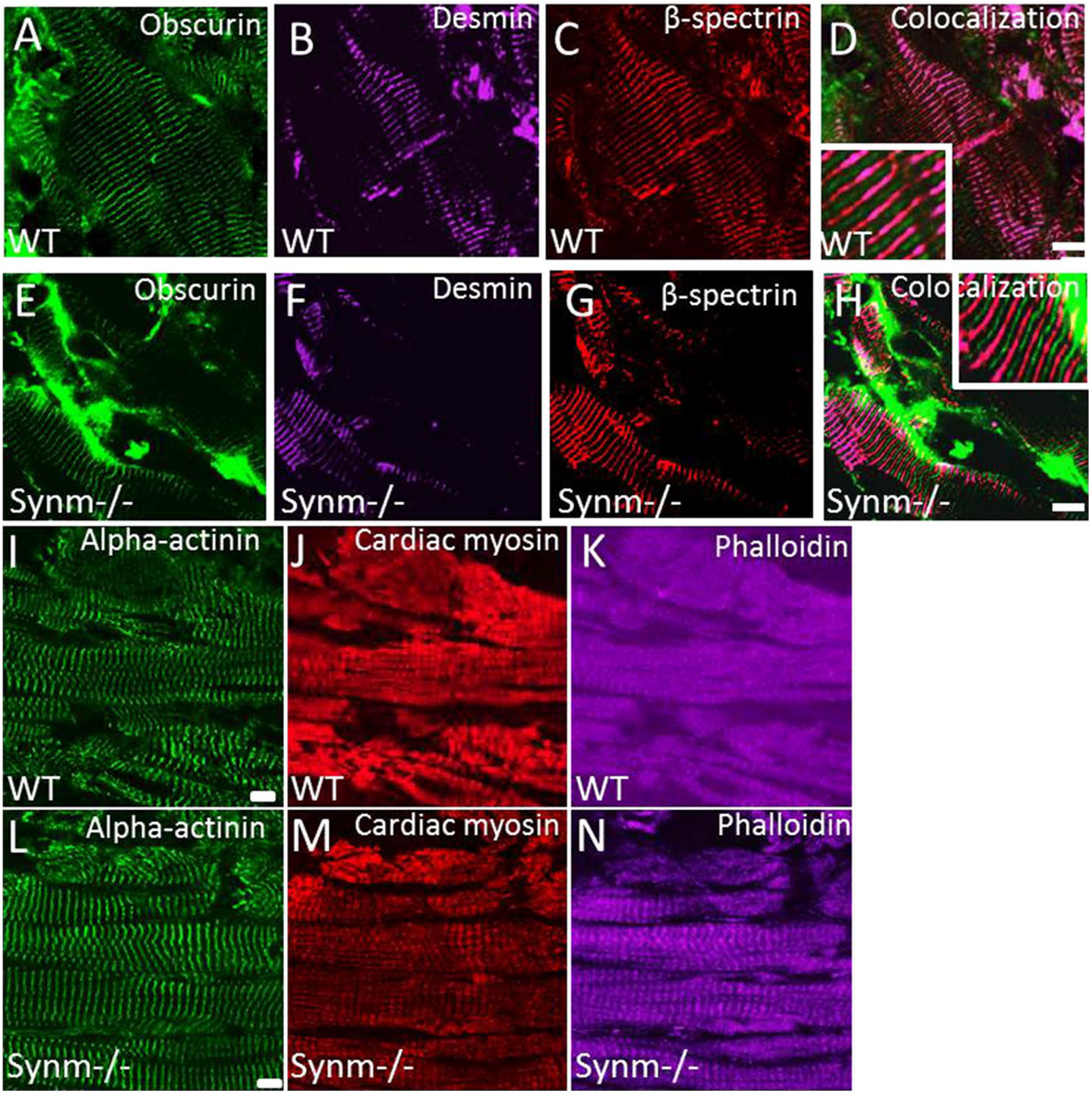

Fig. 6.

Distribution of sarcolemmal and cytoskeletal proteins in cardiac muscle of synm −/− and WT mice (A,N). Frozen longitudinal cryosections of heart from synm-null and WT mice were immunolabeled for obscurin (A,E), desmin (B,F), β-spectrin (C,G), α-actinin (I,L), myosin heavy chain (J,M), and with fluorescent phalloidin (K,N). All structures appear similarly in WT and synm-null heart muscles. Scale bars =10 μm. Insets are enlarged 2.5×.

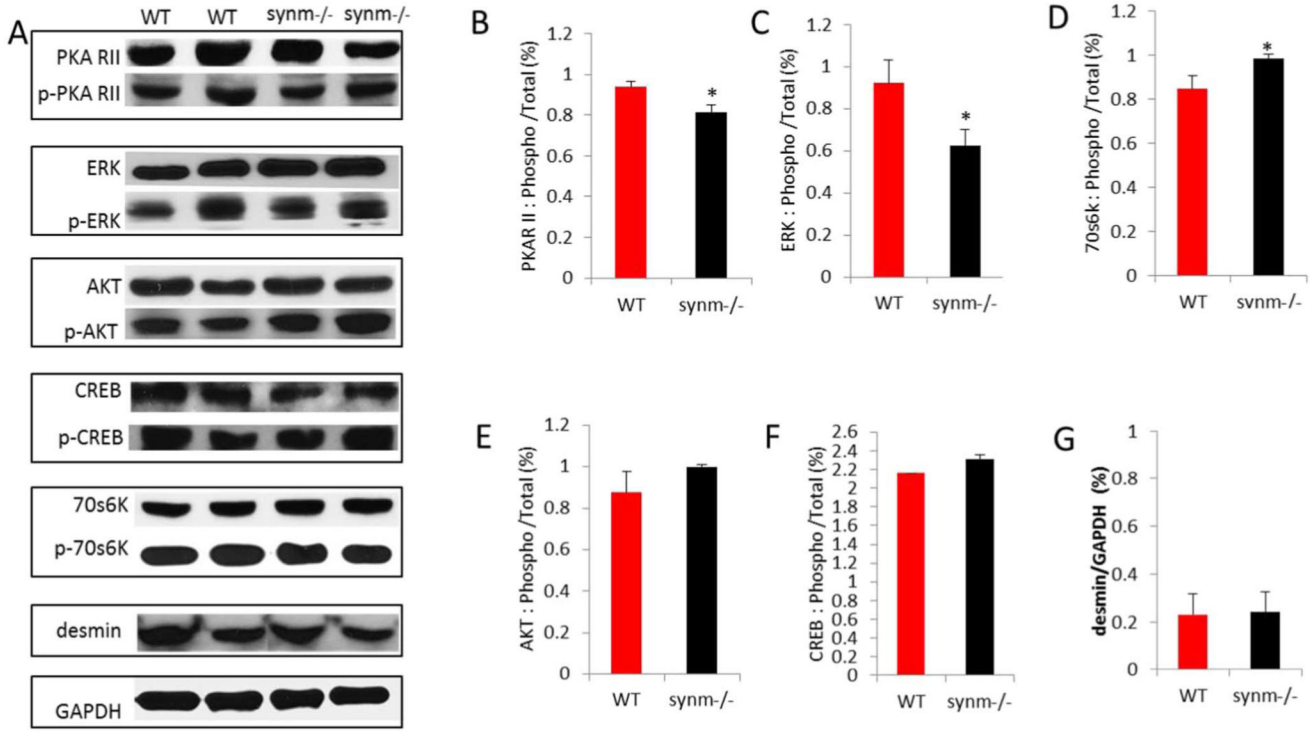

Fig. 7.

Changes in phosphorylation of signaling proteins in synm −/− heart muscle. Western blot assays were performed for 5 signaling proteins and their phosphorylated derivatives and for desmin (A). Phosphorylated forms of PKAR II (B) and ERK1/2 (C) decreased relative to their unphosphorylated forms in synm-null heart. By contrast, p70S6K increased relative to 70S6K (D). There was a trend to higher phosphorylation levels for AKT (E) and CREB (F) in synm −/− mice, but these differences were not significant. Differences in desmin were not significant (G). *$p < 0.05$.